(*23*) could be used in conjunction with this method to guide core biopsies of breast masses. Or, a separate removable device that can be fixed to a PET, SPECT or gamma camera bed could be fabricated. The latter approach would enable these pre-existing devices to be temporarily converted to emission-guided biopsy machines.

CONCLUSION

A simple method for calculation of the position of radionuclide-avid tumors or other photon-emitting bodies utilizing two views from tomograph sinograms has been proposed and experimentally validated. This method has been used to accurately and precisely calculate the position of spheres containing either single-photon or positron-emitting radionuclides. Furthermore, the biopsy of simulated radiopharmaceutical-avid breast lesions was investigated and proven feasible. The excellent results obtained from these experiments indicate that future clinical evaluation of this biopsy method are warranted, especially in situations where anatomical imaging methods are unrevealing.

ACKNOWLEDGMENTS

This work was supported in part by grants CA 53172, and CA 52880 from the National Cancer Institute, Bethesda, MD. Presented in part at the 1995 Society of Nuclear Medicine Meeting, Minneapolis, MN.

REFERENCES

1. Wahl RL, Hutchins GD, Buchsbaum DJ, et al. Fluorine-18-2-deoxy-2-glucose uptake into human tumor xenografts. *Cancer* 1991;67:1545–1550.
2. Wahl RL, Cody RL, Hutchins GD, Mudgett EE. Primary and metastatic breast carcinoma: initial clinical evaluation with PET with radiolabeled glucose analog 2-[^{18}F]-fluoro-2-deoxy-d-glucose. *Radiology* 1991;179:765–770.
3. Tse NY, Hoh CK, Hawkins RA, et al. The application of positron emission tomography imaging with fluoro-deoxyglucose to the evaluation of breast disease. *Ann Surgery* 1992;216(1):27–34.
4. Niewig OE, Kim EE, Wong W-H, et al. Positron emission tomography with fluorine-18-deoxyglucose in the detection and staging of breast cancer. *Cancer* 1993;71:3920–3925.
5. Adler LP, Crowe JJ, Al-Kaise NK, Sunshine JL. Evaluation of breast masses and axillary lymph nodes with [^{18}F]2-deoxy-2-fluoro-d-glucose. *Radiology* 1993;187:743–750.
6. Wahl RL, Helvie MA, Chang AE, Andersson I. Detection of breast cancer in women after augmentation mammoplasty using fluorine-18-fluorodeoxyglucose PET. *J Nucl Med* 1994;35:872–875.
7. Khalkhali I, Mena I, Diggles L. Review of imaging technique for the diagnosis of breast cancer: a new role of prone scintimammography using technetium-99m-sestamibi. *Eur J Nucl Med* 1994;21:357–362.
8. Kao CH, Wang SJ, Liu TJ. The use of technetium-99m-methoxyisobutylisonitrile breast scintigraphy to evaluate palpable breast masses. *Eur J Nuc Med* 1994;21:432–436.
9. Khalkhali I, Mena I, Jouanne E, et al. Prone scintimammography in patients with suspicion of carcinoma of the breast. *J Am Coll Surg* 1994;178:491–497.
10. Heywang-Köbrunner SH. *Contrast-enhanced MRI of the breast.* New York: Basel; 1990.
11. Heywang-Köbrunner SH, Huynh AT, Vichweng P, et al. Prototype breast coil for MR-guided needle localization. *J Comp Assist Tomogr* 1994;18:876–881.
12. Dowlatshahi K, Gent HJ, Schmidt R, Jokich PM, Bibbo M, Sprenger E. Nonpalpable breast tumors: diagnosis with stereotaxic localization and fine-needle aspiration. *Radiology* 1989;170:427–433.
13. Parker SH, Lovin JD, Jobe WE, et al. Stereotaxic breast biopsy with a biopsy gun. *Radiology* 1990;176:741–747.
14. Sullivan DC. Needle core biopsy of mammographic lesions. *Am J Roentgenol* 1994;162:601–608.
15. Fornage BD, Sneige N, Faroux MJ, Andry E. Sonographic appearance of and ultrasound-guided fine-needle aspiration biopsy of breast carcinoma smaller than 1 cm^3. *J Ultrasound Med* 1990;9:559–568.
16. Parker SH, Jobe WE, Dennis MA, et al. US-guided automated large-core breast biopsy. *Radiology* 1993;187:507–511.
17. Sneige N, Fornage BD, Saleh G. Ultrasound-guided fine-needle aspiration of nonpalpable breast lesions. *Am J Clin Pathol* 1994;102:98–101.
18. Saw CB, Ayyongan K, Suntharalingan S. Coordinate transformations and calculation of the angular and depth parameters for a stereotactic system. *Med Phys* 1987;14:1042–1044.
19. Levivier M, Goldman S, Bidaut L, et al. Positron emission tomography-guided stereotactic brain biopsy. *Neurosurgery* 1992;31:792–797.
20. Alexander III E, Loeffler JS, Schwartz RB, et al. Thallium-201, technetium-99m-HMPAO SPECT imaging for guiding stereotactic craniostomes in heavily irradiated malignant glioma patients. *Acta Neurochir (Wien)* 1993;122:215–217.
21. Khalkhali I, Cutrone J, Mena I, et al. Technetium-99m-sestamibi scintimammography of breast lesions: clinical and pathological follow-up. *J Nucl Med* 1995;36:1784–1789.
22. Mena F, Mena I, Diggles L. Design and assessment of scintigraphy guided stereotaxic localization techniques of breast tumors. *J Nucl Med* 1994;35:62P (abstract).
23. Thompson CJ, Murthy K, Weinberg IN, Mako F. Feasibility study for positron emission mammography. *Med Phys* 1994;21:529–538.

Three-Dimensional Bone Scintigraphy Using Volume-Rendering Technique and SPECT

Toyotsugu Ota, Itsuo Yamamoto, Hideo Ohnishi, Itsuaki Yuh, Yusuke Kigami, Teruyasu Suzuki, Yasuyo Yamamura, Kiyoshi Murata and Rikushi Morita

Department of Radiology, Shiga University of Medical Science, Seta, Otsu, Shiga, Japan

Three-dimensional bone scintigraphic images were made and their usefulness and limitations discussed. **Methods:** After usual bone scan procedures, single-photon emission computed tomography (SPECT) data were taken and reconstructed into three-dimensional images. Volume rendering methods were used. **Results:** Three cases of three-dimensional bone scintigraphy were obtained; one of a normal patient, one of a case of transplanted kidney and incomplete fracture of the left femoral head, and one of a case of degenerative joint disease (DJD) on the left temporomandibular joint (TMJ). The three-dimensional structure of the skeletal system was depicted more clearly by the three-dimensional images than by a conventional bone scan. **Conclusion:** Three-dimensional bone scintigraphs were thought to provide additional information for better understanding of the nature of bone lesions. Some technical improvements including automated threshold level determination and feature extraction for detecting abnormal high uptake are required before routine use can be envisaged.

Key Words: three-dimensional imaging; bone scintigraphy; SPECT; volume rendering

J Nucl Med 1996; 37:1567–1570

Recently, reconstruction techniques for three-dimensional imaging have made remarkable progress and are being applied to various modalities, such as CT, MRI and some scintigraphies. Some of them are already being utilized in bedside

Received May 15, 1995; revision accepted Sept. 12, 1995.

For correspondence or reprints contact: Toyotsugu Ota, MD, Department of Radiology, Shiga University of Medical Science, Seta, Otsu, Shiga, 520-21, Japan.

A

0	5	12	16	13	1
3	2	25	26	15	4
8	16	30	35	15	11
4	13	14	25	18	16
2	8	12	15	16	15
1	3	9	14	9	8

B

0	0	50	50	50	0
0	0	100	100	50	0
0	50	100	100	50	50
0	50	50	100	50	50
0	0	50	50	50	50
0	0	0	50	0	0

FIGURE 1. Example of segmentation of voxel value. (A) Original SPECT data and (B) segmented data ("match mark data") in which levels 1 and 2 were set to 10 and 20, respectively.

practice. These display techniques can show the exact location of the lesion in relation to normal anatomical structure, which establishes their clinical utility (*1–4*).

METHODS

Conventional bone scintigrams were obtained with a dual whole-body scinticamera using ^{99m}Tc-hydroxy-methane-diphosphonate (HMDP) in patients with various skeletal disorders. After usual bone scan procedures, projection images were obtained by a rotating scinticamera with an acquisition matrix size of 128 × 128, and pixel size of 4 mm, gapless. A low-energy, high-resolution (LEHR) collimator with a 5.7 mm FWHM was used. Sixty rotation angles were used with 6° per view. Each view took 20 sec; whole-body scanning took 22 min. Transaxial SPECT images were reconstructed using a Butterworth prefilter (*5*) (cutoff frequency 0.1 cycles/pixels) and ramp backprojection and transferred to a Titan750V (Kubota Computer Inc., Tokyo, Japan) via a VAX8250 (Digital Equipment Corp., Maynard, MA). On the Titan750V, SPECT data of 128 × 128 × 128 voxels were magnified into 255 × 255 × 255 voxel data using a self-made program written in C which includes a linear interpolation process. No other smoothing technique was applied to the images. Thereafter, one or two threshold level(s) were determined manually to segment the SPECT data: level 1 to depict the normal bones and level 2 to depict lesions with higher uptake. The levels were determined by trial and error. Voxels with a value of ≤level 1 were standardized to a value of zero; those between levels 1 and 2, fifty; the rest, a hundred, to make what we call "match mark" data (Fig. 1). With the software "Volume Design (Medical Design, Tokyo, Japan)" on the Titan 750V, these "match mark" data were reconstructed into three-dimensional images using a volume rendering method. For Patient 1 (Fig. 2), opacity was set to 100%, that is, the pictures were equal to surface-rendering pictures. On the other hand, opacity was set to 70% in Patients 2 and 3 (Figs. 3 and 4) so that

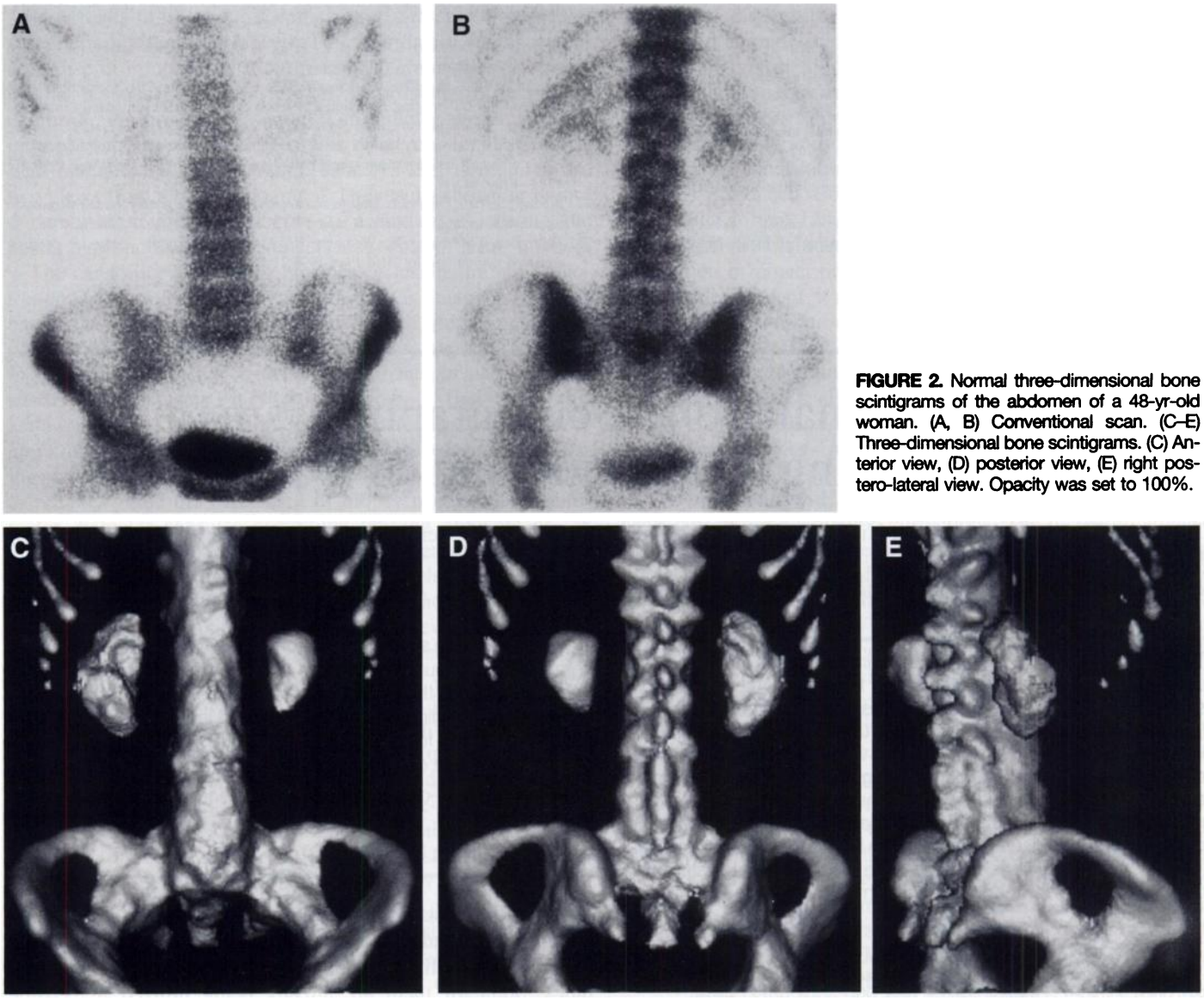

FIGURE 2. Normal three-dimensional bone scintigrams of the abdomen of a 48-yr-old woman. (A, B) Conventional scan. (C–E) Three-dimensional bone scintigrams. (C) Anterior view, (D) posterior view, (E) right postero-lateral view. Opacity was set to 100%.

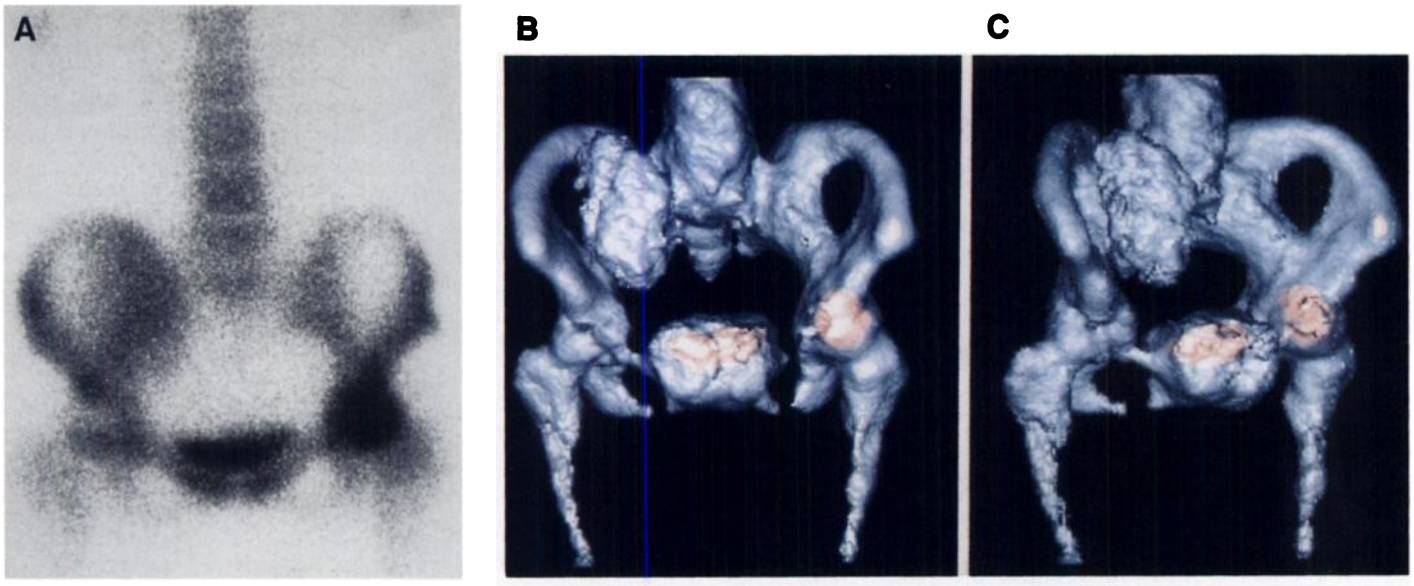

FIGURE 3. Pelvic bone scan of a 26-yr-old woman who underwent kidney transplantation. Kidney mimicks abnormal uptake in the right iliac bone in conventional bone scan (A), while three-dimensional scan (B, C) fairly differentiates them. This patient also has an incomplete fracture of the left femoral head possibly related to steroid therapy. Lesion is depicted in red and can be seen through the normal bone. Left hip joint is somewhat "swollen," another manifestation of the hot spot in this method. Opacity of bones was set to 70%, slightly transparent.

the pictures were slightly transparent, making red-colored hot spots visible from outside.

RESULTS

Figure 2 shows the normal bone scan images of a 48-yr-old woman complaining of lumbago who had a history of breast cancer. In this patient, only level 1 was set to the "match mark" data. Compared to conventional bone scans (Fig. 2A, B), three-dimensional bone scintigrams (Fig. 2C, D, E) clearly depicted the three-dimensional structure of the lower vertebral and pelvic skeletal system. Identification of the skeletal components, such as the transverse process, spinous process and sacrum, is easier on the three-dimensional images than on the planar images. Figure 3 shows a pelvic bony system with a transplanted kidney in the right pelvic region of a 26-yr-old woman. The kidney mimics increased tracer uptake in the right iliac bone on the classic bone scintigrams (Fig. 3A), but they are easily differentiated from each other on the three-dimensional images (Fig. 3B, C). Abnormal accumulation of the radionuclide in the left femoral head due to incomplete fracture is easily differentiated from the normal uptake by the hip joint areas. This abnormality was depicted also as an increase in volume; the left hip joint is somewhat swollen both in the two-dimensional and three-dimensional pictures (Fig. 3). Figure 4 shows the two-dimensional and three-dimensional images of the skull of a patient with the left temporomandibullar joint (TMJ) degenerative joint disease (DJD). The area of high tracer uptake by the left TMJ is depicted in red on the three-dimensional images. Other areas with higher uptake in the skull base, maxilla and vertebral bodies are interpreted as normal findings.

DISCUSSION

Radionuclide bone scanning is now widely accepted as a major clinical procedure because of its high sensitivity in detecting early bone diseases prior to radiographic or enzymic changes, very low false-negative rates, reproducibility and suitability as a screening procedure, low radiation exposure and so on (*6,7*). Understanding of the precise structure of the bony systems and pathological lesions is not always easy due to

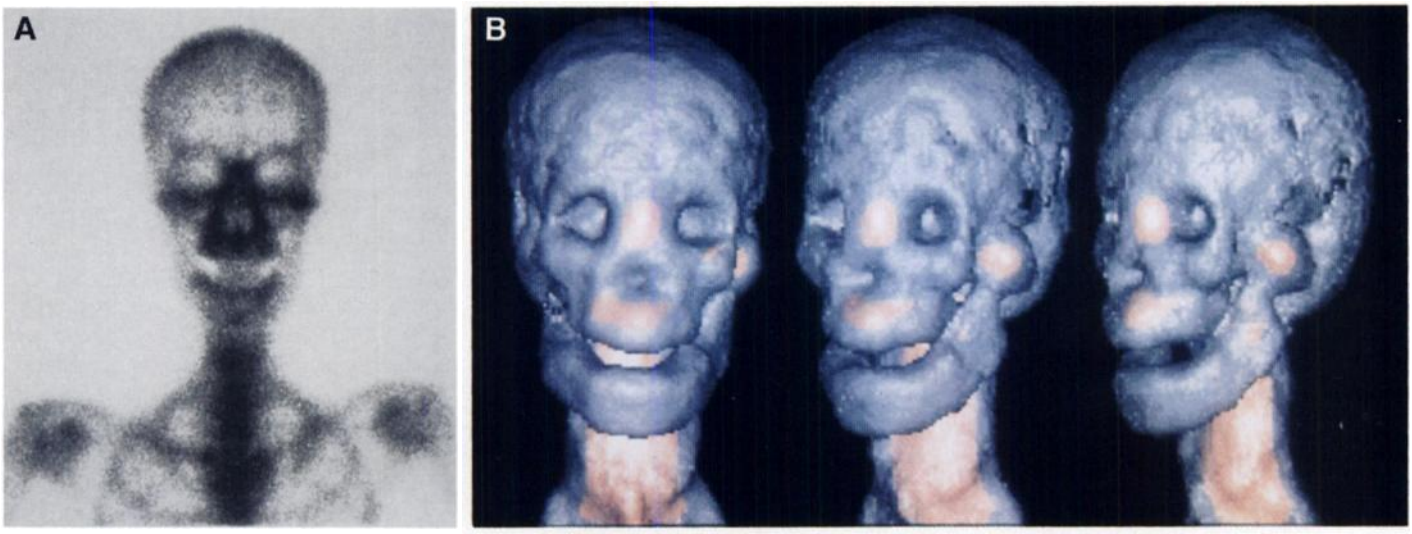

FIGURE 4. A 59-yr-old woman with DJD on the left temporomandibullar joint. Lesion is delineated in red in the three-dimensional pictures (Fig. 4B). Other areas colored in red are naturally high uptake portions (normal finding).

relatively poor spatial resolution. On the other hand, three-dimensional display techniques have recently developed rapidly and are now applied to a variety of imaging techniques for almost all parts of the body: the musculoskeletal system, central nervous system, cardiovascular system, pulmonary system, and gastrointestinal and genitourinary systems (*3,4*). The main advantage of using three-dimensional images is that the spatial relationships of the objects are easily recognizable. We realize that anatomically meticulous three-dimensional images of the skeletal system can be obtained from x-ray computed tomography (CT). In particular, spiral (helical) x-ray CT offers almost true-to-life images. X-ray CT images are low-noise, linearly related to tissue electron density, with density and spatial resolutions on the order of 1% and 1 mm, respectively: radioisotope images are inherently noisier and of lower spatial resolution, although several techniques have been studied to improve them (*3,5*). PET images have advantages over conventional radioisotope images for their high spatial resolution, and the use of a bone-seeking positron emitter such as [^{18}F]fluoride would provide successful three-dimensional bone images. The exigencies of the PET machine and cyclotron, however, hamper their widespread application in clinical work. These facts may have made investigators reluctant to study three-dimensional bone scintigraphy.

Application of Three-Dimensional Imaging to Bone Scan

The effectiveness of diagnostic imaging, however, depends not only on the precision of the morphology but also on sensitivity to the biological functions. Bone scintigraphy is the only current method to reflect osteoblastic activity of the skeleton with high sensitivity and specificity. The addition of the morphological element by three-dimensional images to bone scintigraphy, which inherently possesses the functional element, would promote its role in the evaluation of bone diseases. Some bone diseases, including metabolic bone diseases, can be detected by bone scans at an early stage when conventional radiography shows no abnormality. Bone scintigraphy can provide functional images combined with structure. By making the morphology more recognizable, we will obtain more information about the patient. In our method, no other radionuclides are administered to patients to obtain three-dimensional images after conventional bone scanning. Given that radioisotope examinations subject patients to low radiation exposure, bone scintigraphy enables two-dimensional images as well as supplementary three-dimensional information of the bony system without additional radiation exposure to the patient. In this study, we set two threshold levels for stratifying the magnitudes of the accumulation of the radionuclide: one (level 1) to depict normal bones, the other (level 2) for the higher uptake portion. According to the classification of three-dimensional images by Wallis and Miller (*8*), this method is of the "Full segmentation, Illuminated type."

Normal versus Abnormal High Uptake and Cold Spots

There are some portions of the body in which tracer uptake is basically high, such as the skull base, vertebral body and so on. It seems difficult to differentiate abnormal from normal high uptake, but our data allowed us to distinguish it in some patients. In Figure 4, for example, we recognize that three portions with higher tracer uptake than the upper threshold—the skull base, maxillas and vertebral bodies—are normal where tracer uptake is naturally high. On the contrary, high tracer uptake by the left TMJ is easily discernible as pathological, given that this is not a place where normally increased uptake would be seen. Asymmetry is another clue in this patient, a factor that is not applicable for all patients.

Defining a region of interest is a profound problem shared by all three-dimensional scintigraphic images (*9*). Our images are not exceptions. Scans made with our method seem to have the following problems:

1. Some skill is required to distinguish abnormal from normal high uptake.
2. Images do not visualize cold spots as in other three-dimensional scintigraphic studies.
3. Our method masks hot spots in areas where uptake is normally high.

An automated feature extraction system that could differentiate abnormally high lesion uptake from normal uptake would solve these problems and will be incorporated in future studies of our method to improve image quality.

CONCLUSION

We constructed three-dimensional bone scan images from the usual SPECT data and demonstrated that three-dimensional bone imaging is a practical and accessible approach that improves orientations of anatomically three-dimensional bone structure. Further development of automated reconstruction and feature-extracting software should enable routine use of three-dimensional bone scanning.

REFERENCES

1. Hemmy DC, Zonneveld FW, Lobregt S, Fukuta K. A decade of clinical three-dimensional imaging: a review, part one. *Invest Radiol* 1994;29:489–496.
2. Zonneveld FW, Fukuta K. A decade of clinical three-dimensional imaging: a review, part two. *Invest Radiol* 1994;29:574–589.
3. Webb S, Ott RJ, Flower MA, McCready VR, Meller S. Three-dimensional display of data obtained by single photon emission computed tomography. *Br J Radiol* 1987;60: 557–562.
4. Herman GT. 3D display: a survey from theory to applications. *Comp Med Imag Graph* 1993;17:231–242.
5. Brown ML, O'Connor MK, Hung JC, Hayostek RJ. Technical aspects of bone scintigraphy. *Radiol Clin North Am* 1993;31:721–730.
6. Ell PJ. Bones and joints. In: Maisey MN, Britton KE, Gilday DL, eds. *Clinical nuclear medicine* London: Chapman and Hall Ltd; 1983:135–165.
7. Holder LE. Clinical radionuclide bone imaging. *Radiology* 1990;176:607–614.
8. Wallis JW, Miller TR. Volume rendering in three-dimensional display of SPECT images. *J Nucl Med* 1990;31:1421–1428.
9. Keyes Jr JW. Three-dimensional display of SPECT images: advantages and problems [Editorial]. *J Nucl Med* 1990;31:1428–1430.